



Energy Analysis of Lateral vs. Normal Vibration Modes for Ultrasonic Surface Haptic Devices

Diana Angelica Torres Guzman^(✉), Betty Lemaire-Semail,
Frederic Giraud, Christophe Giraud-Audine, and Michel Amberg

Univ. Lille, Arts et Metiers Institute of Technology, Centrale Lille,
Yncrea Hauts de-France, L2EP – ULR 2697, 59000 Lille, France
diana.torres-guzman@univ-lille.fr

Abstract. In this paper, we propose a new device in order to produce normal and lateral ultrasonic vibrations in a plate, using an array of piezoelectric ceramics. This setup serves to continue the comparative analysis between the two vibration modes for tactile feedback rendering, by including an energetic characterization. With the help of a tribological analysis, this study will help to examine the energy performance of each vibration mode in terms of active power consumption against friction contrast (which is linked to perception). Using a simplified second order plate model, the energetic results are analyzed. The results show a better energy efficiency for the lateral vibration for low exploration speeds. The tribological analysis helps as well to evaluate the effect of frequency increase in terms of friction reduction vs. vibration amplitude for both vibration modes.

Keywords: Surface haptics · Ultrasonic · Out of plane vibrations · Lateral vibration · Friction reduction · Power measurement

1 Introduction

Haptic devices for texture discrimination utilize techniques to achieve friction modulation, since differences in friction may create a perception of texture [1]. In order to achieve this, ultrasonic vibration may be used to produce friction reduction on a surface, thus creating a sensation of ‘smoothness’ [2] (active lubrication). The amount of friction reduction is dependent on the vibration amplitude and frequency [3], and properties of the probing object [4, 5].

Generally, ultrasonic tactile feedback surfaces use out of plane vibration. However, lateral modes for friction reduction may also be interesting for several purposes, such as mechanical integration and noise reduction, and may be used additionally or in place of normal modes. The phenomenon of friction reduction with ultrasonic vibration has been thoroughly explored for ‘out-of-plane’ [6–9], or for combined vibration modes [10]. But the interaction mechanism through which friction is reduced with purely lateral vibration is less explored.

In [6], a simplified finger model, is used to explore the effects of lateral ultrasonic vibration on the grip function. In [7] this model is used to analyze the comparison

between lateral and normal vibration modes, by measuring the perception of friction contrast for each mode at a set of vibration amplitudes, for a group of participants. With the test conditions explained in [7], the psychophysical measures indicate that the large majority of subjects are more sensitive to normal rather than lateral vibration modulation for a given value of wave amplitude, up to about $3 \mu\text{m}_{\text{p-p}}$, at frequencies around 30 kHz. The measurements have also shown that the finger exploration speed affects significantly the result with lateral vibration, requiring larger amplitudes at higher speeds to produce the same perception.

The energetic performance could also be a determinant factor in the mode choice for haptic devices. Indeed, if the haptic device is to be used with a battery, for example, a better energetic performance may help increasing operational time or reducing battery capacity specifications.

It is therefore interesting to evaluate the energetic requirement for a given friction contrast ($\Delta\mu/\mu$: where $\Delta\mu$ is equal to the friction coefficient without vibration (μ) minus the friction coefficient with vibration), for a given subject, since this value is related to perception [8]. In order to do so, a new device has been conceived and built. This device allows exciting either a normal or a lateral mode (at similar frequencies), with a same set of piezo-ceramics. Two experiments are then designed, for both vibration modes. In the first one, the active power required to reach a given vibration amplitude is measured, with and without load (finger). The second experiment consists of a tribology analysis, which serves to link the vibration amplitude with the friction modulation. Additionally, the tribology analysis will help studying the effect of increasing the frequency, in comparison with the results presented in [7], and knowing whether the exploration speed continues to influence the result.

Section 2 explains the conception and setup of the ultrasonic device. The lateral and normal modes created in this device are characterized and evaluated in terms of energy vs. vibration amplitude in Sect. 3, while Sect. 4.

2 Device Producing Lateral and Normal Modes on a Plate

A new ultrasonic device is designed to produce a pure lateral mode and a normal mode vibration on the same structure, with the same motion sources. The resonance frequencies of both modes must be close to each other without causing interference, and they must be higher than 30 kHz, which is the frequency already tested in [7], in order to explore the effect of increasing frequency on lateral haptic devices. For this reason, the design is made at about 60 kHz.

The conceived structure consists of an aluminum plate with twelve piezoelectric ceramics glued to the center of the plate on both sides (see Fig. 1), similar to the setup proposed in [11]. Ten of these ceramics serve as actuators, and two are sensors. A damp-proof polymeric material is glued to the top face of the aluminum beam on both sides. This design allows an exploration area through a length of about 3 cm between two nodes. The dimensions of the resonator are 128 mm \times 30 mm \times 1.94 mm, and the ceramics are 5 mm \times 9 mm \times 0.3 mm. The resonator is attached to an immobile section through a series of isthmus situated approximately at the vibrational nodes of both modes.

An optimization algorithm is performed in order to estimate the dimensions which may minimize the difference between the resonance frequencies of the two modes, without having them interfere with each other, as they are meant to be comparable but excited independently. It is important to mention that the device is not created to be optimal in terms of energy consumption, as in [11, 12], but built in such a way as to render the two modes comparable. Once these dimensions are estimated, a modal analysis is performed using finite element analysis. The results of the analysis will help calculating in precision the geometry of the device and the placement of the piezo-ceramics.

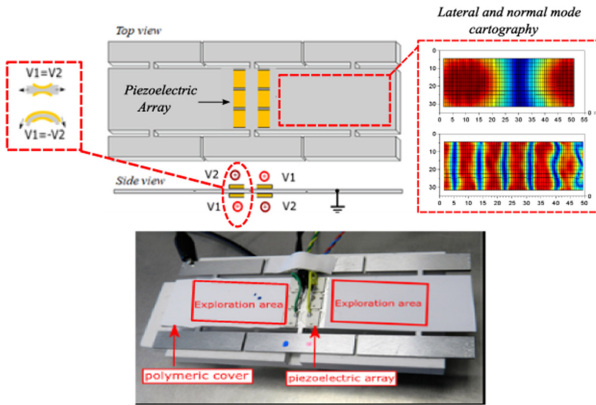


Fig. 1. Plate design and setup to perform mode comparison on the same surface haptic device. At top right, the cartography of lateral (up) and normal (down) modes on one side. The cartography confirms that the modes are almost completely pure. The scanned area does not include the portion with the ceramics, which is why nodal lines look asymmetrical.

The ‘top’ and ‘bottom’ side ceramics are connected to different voltage sources (V_1 and V_2 on Fig. 1), with the common ground connected to the conductive plate. All ceramics deform in a d_{31} mode (stretch-compress), creating a surface tension on the aluminum surface. When $V_1 = V_2$, a symmetrical stretch-compress deformation is produced simultaneously on both sides of the aluminum plate, thus inducing the lateral mode. When $V_1 = -V_2$, one surface will be stretched, while the other compressed, ‘bending’ the material, thus inducing the normal mode. This method allows creating relatively pure lateral and normal modes.

3 Energy Analysis

3.1 Dynamic Model of the Plate at no-Load Condition

In order to explain the differences we observe with the two vibration modes, let us come back to the mechanical behavior of the plate. As it has been explained in [13], the dynamics of a device at resonance can be simplified as a second order model (1).

$$M_{L/N}\ddot{w} + D_{L/N}\dot{w} + K_{L/N}w = N_{L/N}V \quad (1)$$

The index L/N indicates that the equation is accurate for both lateral and normal modes. Assuming that a single mode is being excited at its resonance frequency, this equation serves to represent the modal parameters of mass $M_{L/N}$, dampening $D_{L/N}$, and elasticity $K_{L/N}$. The state variables w , \dot{w} and \ddot{w} , represent the instantaneous displacement, speed and acceleration, respectively. Since the motion source is a piezoelectric ceramic, the electrical part of the equation, representing the motion force from the piezoelectric transducer, may be written as $N_{L/N}V$, with $N_{L/N}$ representing the electro-mechanical transformation factor, and V value of the input voltage. The parameters of the plate are identified experimentally, as described in [14], with 40 V pk-to-pk applied to the lateral mode, and 12 V pk to pk to the normal mode. Their values are listed in Table 1. The question of the voltage difference will be addressed in Sect. 5.

Table 1. Modal parameters identified for the lateral and normal modes induced on the device

| Parameter | Mode | Symbol | Value |
|--|---------|--------|------------|
| Electro-mechanical transformation factor | Lateral | N_L | 0.0773 N/V |
| Modal Mass | Lateral | M_L | 15.4 g |
| Modal Dampening | Lateral | D_L | 27 N s/m |
| Modal Elasticity | Lateral | K_L | 2017 MPa |
| Electro-mechanical transformation factor | Normal | N_N | 0.3 N/V |
| Modal Mass | Normal | M_N | 13.8 g |
| Modal Dampening | Normal | D_N | 22.1 N s/m |
| Modal Elasticity | Normal | K_N | 1678 MPa |

3.2 Active Power Measurement

In order to measure the active power consumption, a Fluke Norma 4000 power analyzer is connected to the motor ceramics. A frequency sweep is made at about ± 1 kHz around the resonance at three different voltage amplitudes. The voltages are set for each mode to produce a vibration amplitude at resonance of $0.8 \mu m_{p-p}$, $0.6 \mu m_{p-p}$ and $0.3 \mu m_{p-p}$. The vibration amplitude values are recorded together with the total active power measurement for each frequency. The measurements are performed three times: first at no load, then with a static finger pressing over the surface at a normal force of 0.5 N, and finally with a finger pressing at 1 N. The results are shown in Fig. 2.

The normal and lateral modes show a similar behavior with the power evolving proportionally to the square of the amplitude at no load. For these conditions, the lateral mode requires marginally less power for a given wave amplitude. It is also possible to observe that the presence of the finger produces an attenuation of the amplitude, and a slight shift of the resonance frequency. These phenomena impact more significantly the normal mode, with an attenuation of over 54%, against 23% for the lateral mode. In Fig. 2, it can be perceived that with a load, the power required to achieve a given

amplitude is increased. An interpolation of the evolution of the power vs. amplitude at resonance can be made for each curve, with a quadratic fit of the measured data. This result (see Fig. 3) provides a relation of the wave amplitude versus active power for each studied case.

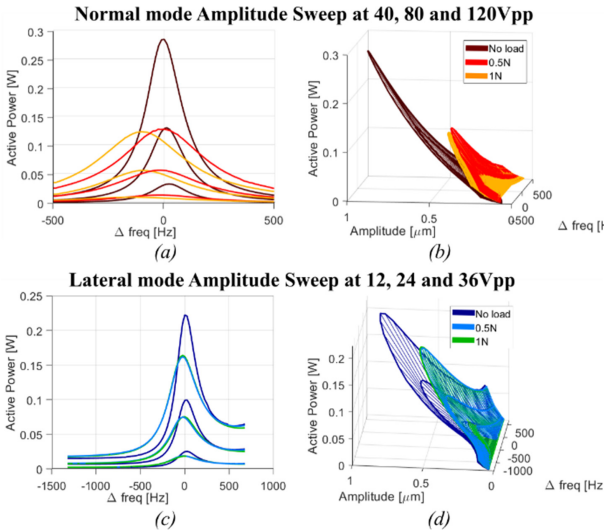


Fig. 2. Active Power for a frequency sweep for normal and lateral modes, for three voltage supplies and three finger pressures. (a) and (c) Amplitude vs. frequency shift. The graph shows the attenuation due to a finger pressing on the surface. (b) and (d) Power vs. Amplitude.

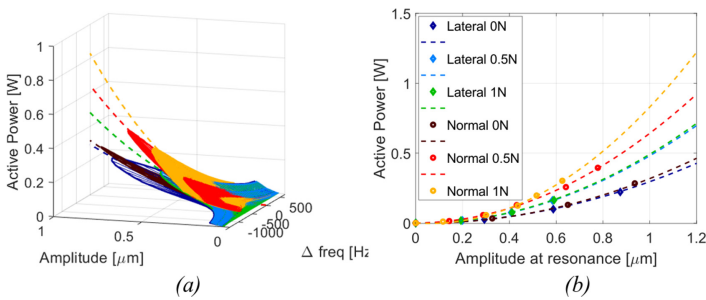


Fig. 3. Active power vs. amplitude, relation extrapolation. (a) Evolution of power vs. amplitude at resonance from the sweep data. (b) Power vs. Amplitude relation vs. the points for the measured data at resonance. The quadratic fit of the lateral power measurements at loads of 0.5 N and 1 N are superposed.

4 Tribology Analysis

4.1 Frequency and Speed Effects for a Hard Probe and for a Finger

In order to compare the friction reduction for both modes at different frequencies, the relative friction coefficient $\mu' = \mu_k / \mu_0$ (with μ_k a measurement at a given amplitude, and μ_0 the measurement without vibration) is deduced thanks to a tribometer, either using an artificial finger (a probe already used in [7]), or with a real finger.

The measurements are performed for different finger or probe speeds, and for the two vibration modes. These results will allow determining the relation of active power vs. friction reduction for each mode. The mechanism through which friction is reduced with purely lateral modes is explained in [7], based on the model proposed in [6] (Fig. 4).

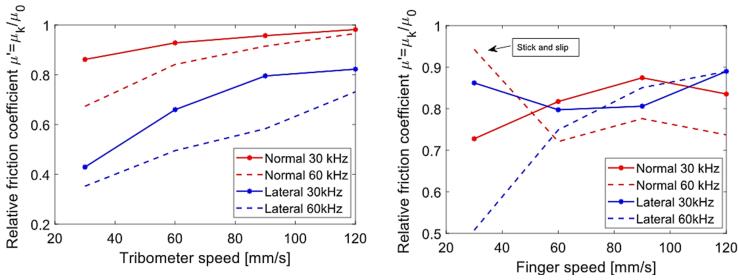


Fig. 4. Tribology measurements at 30 kHz vs. 60 kHz, at a vibration amplitude of $1.2 \mu\text{m}_{\text{p-p}}$, and a pressing force of 0.5 N. Left: Tribometer measurements. Right: mean value of the measurements on a moving finger. Stick and slip was felt by the finger for normal vibration with a speed of 30 mm/s, which may explain the relatively high measurement. Moreover, active exploration with a moving finger may produce inaccuracies in the friction measurement of up to ± 0.2

The tribology results are compared with results gotten with the devices previously used in [7]. These devices worked at a resonance frequency about 30 kHz. At the same exploration speed, the same vibration amplitude ranges, the same probe and the same finger, this comparison allows an analysis of the vibration frequency influence (30 kHz versus 60 kHz). Indeed, the measurements taken with the tribometer at $1.2 \mu\text{m}_{\text{p-p}}$ wave amplitude, show that the increase in frequency improves the lubrication for both modes.

4.2 Active Power vs. Friction Contrast

As the amplitude of vibration increases, so does the friction contrast of the surface with and without vibration. It is possible to use the measured friction data at different amplitudes, and combine it to the amplitude vs. power relation found in Sect. 3.2 (Fig. 3), in order to estimate the actual energy required to produce a given friction contrast on a plate when using either a normal or a lateral mode (see Fig. 5).

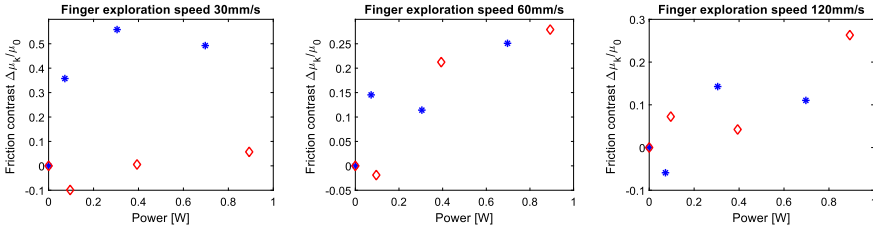


Fig. 5. Friction contrast vs. active power for 30 mm/s, 60 mm/s and 120 mm/s exploration speed. Blue: lateral vibration. Red: Normal vibration. Negative values may be a product of measurement imprecisions, or because of the presence of stick and slip which may increase the friction. (Color figure online)

The results show that, for a frequency about 60 kHz, for slow exploration speeds (30–60 mm/s), the lateral mode shows a better energy performance than the normal devices, for producing a given relative friction contrast in a finger. With higher scanning speeds (60–120 mm/s), normal modes are slightly more advantageous.

5 Discussion

This study utilized the dynamic model of a vibrating plate to analyze the energy performance of the different modes. In Table 1, it can be verified that the mechanical parameters for each mode are different. The identified electro-mechanical transformation factor indicates that the piezoelectric array produces a force about 5.5 larger when ‘bending’ the plate (to produce the normal mode), than when ‘stretching’ it (to produce the lateral mode), since the ceramics are better coupled with this mode. This can be explained by the difference of the wavelength of each mode. This produces a more important deformation of the ceramic in the normal mode than in the lateral mode. It can be seen as well that the damping factor (which is related to active power consumption) of the normal mode is higher than the one for the lateral mode, hence the active power consumption is higher as well.

Thanks to the tribology experiment, it was possible to observe a difference in friction reduction at different finger speeds for the lateral mode at 60 kHz as it is observed for 30 kHz in [6]. It is also confirmed that the frequency increase improves the active lubrication results for both modes. This phenomenon affects more the lateral vibration. For this reason, the relation of amplitude vs. sensation found in [6] may no longer be factual at 60 kHz vibration.

6 Conclusions

In this article, a device was created in order to perform an energetic comparison between two vibration modes at 60 kHz vibration frequency. The active power requirements show that lateral modes are generally advantageous in terms of the energy requirement to reach a given vibration amplitude, especially in the presence of a load.

The presence of the finger affects more significantly one mode than the other. This can be explained by the nature of the contact, a subject which may be explored in further studies.

When comparing the relation of power against friction contrast for both modes, it is the exploration speed which influences most the results. Indeed, at exploration speeds of 30–60 mm/s, the lateral vibration mode appears to require less active power than the normal mode to reach the same friction contrast. It is comparable or slightly worse to the normal mode for higher exploring speeds of 60–120 mm/s.

As a follow-up to this study, a psychophysical test will be performed in order to relate this study with perception for a set of different participants. This will also help evaluate the variability of friction contrast in terms of power from one subject to another.

Acknowledgements. This work is supported by IRCICA (Research Institute on software and hardware devices for information and Advanced communication, USR CNRS 3380).

References

1. Adams, M.J., et al.: Finger pad friction and its role in grip and touch. *J. R. Soc. Interface* **10** (80), 20120467 (2012)
2. Biet, M., Giraud, F., Lemaire-Semail, B.: Squeeze film effect for the design of an ultrasonic tactile plate. *IEEE Trans. Ultrason. Ferroelectr. Freq. Control* **54**(12), 2678–2688 (2007)
3. Sednaoui, T., Vezzoli, E., Dzidek, B., Lemaire-Semail, B., Chappaz, C., Adams, M.: Friction reduction through ultrasonic vibration part 2: experimental evaluation of intermittent contact and squeeze film levitation. *IEEE Trans. Haptics* **10**(2), 208–216 (2017)
4. Friesen, R.F., Wiertelwski, M., Colgate, J.E.: The role of damping in ultrasonic friction reduction. In: *IEEE Haptics Symposium 2016, Philadelphia*, pp. 167–172 (2016)
5. Janko, M., Wiertelwski, M., Visell, Y.: Contact geometry and mechanics predict friction forces during tactile surface exploration. *Sci. Rep.* **8**, 4868 (2018)
6. Vezzoli, E., Dzidek, B., Sednaoui, T., Giraud, F., Adams, M., Lemaire-Semail, B.: Role of fingerprint mechanics and non-Coulombic friction in ultrasonic devices. In: *IEEE World Haptics Conference (WHC) 2016, Evanston, IL*, pp. 43–48 (2015)
7. Torres Guzman, D.A., Lemaire-Semail, B., Kaci, A., Giraud, F., Amberg, M.: Comparison between normal and lateral vibration on surface haptic devices. In: *IEEE World Haptics Conference (WHC) 2019, Tokyo*, pp. 199–204 (2019)
8. Messaoud, W.B., Bueno, M.-A., Lemaire-Semail, B.: Relation between human perceived friction and finger friction characteristics. *Tribol. Int.* **98**, 261–269 (2016)
9. Winfield, L., Glassmire, J., Colgate, J.E., Peshkin, M.: T-PaD: tactile pattern display through variable friction reduction. In: *Second Joint EuroHaptics Conference and Symposium on Haptic Interfaces for Virtual Environment and Teleoperator Systems (WHC 2007), Tsukuba, Japan*, pp. 421–426 (2007)
10. Dai, X., Colgate, J.E., Peshkin, M.A.: LateralPaD: a surface-haptic device that produces lateral forces on a bare finger. In: *IEEE Haptics Symposium (HAPTICS)*, pp. 7–14 (2012)
11. Wiertelwski, M., Colgate, J.E.: Power optimization of ultrasonic friction-modulation tactile interfaces. *IEEE Trans. Haptics* **8**(1), 43–53 (2015)

12. Yang, Y., Lemaire-Semail, B., Giraud, F., Amberg, M., Zhang, Y., Giraud-Audine, C.: Power analysis for the design of a large area ultrasonic tactile touch panel. *Eur. Phys. J. Appl. Phys.* **72**(1), 11101 (2015)
13. Ghenna, S., Giraud, F., Giraud-Audine, C., Amberg, M.: Vector control of piezoelectric transducers and ultrasonic actuators. *IEEE Trans. Ind. Electron.* **65**(6), 4880–4888 (2018)
14. Giraud, F., Giraud-Audine, C.: *Piezoelectric Actuators: Vector Control Method*, 1st edn. Elsevier, Cambridge (2019)

Open Access This chapter is licensed under the terms of the Creative Commons Attribution 4.0 International License (<http://creativecommons.org/licenses/by/4.0/>), which permits use, sharing, adaptation, distribution and reproduction in any medium or format, as long as you give appropriate credit to the original author(s) and the source, provide a link to the Creative Commons license and indicate if changes were made.

The images or other third party material in this chapter are included in the chapter's Creative Commons license, unless indicated otherwise in a credit line to the material. If material is not included in the chapter's Creative Commons license and your intended use is not permitted by statutory regulation or exceeds the permitted use, you will need to obtain permission directly from the copyright holder.

